Crystal structure, magnetic and electrical properties of the $Nd_{1-x}Ba_xCoO_3$ system

2005 J. Phys.: Condens. Matter 17 4181

(http://iopscience.iop.org/0953-8984/17/26/016)

INSTITUTE OF PHYSICS PUBLISHING JOURNAL OF PHYSICS: CONDENSED MATTER

J. Phys.: Condens. Matter **17** (2005) 4181–4195 doi:10.1088/0953-8984/17/26/016

Crystal structure, magnetic and electrical properties of the $Nd_{1-x}Ba_xCoO_3$ system

A P Sazonov[1,6], I O Troyanchuk[1], V V Sikolenko[2,3], G M Chobot[4] and H Szymczak[5]

[1] Institute of Solid State and Semiconductor Physics, National Academy of Sciences, P Brovka Street 17, BY-220072 Minsk, Belarus
[2] Berlin Neutron Scattering Center, Hahn-Meitner-Institut, D-14109 Berlin, Germany
[3] Joint Institute for Nuclear Research, 141980 Dubna, Moscow Region, Russia
[4] Belarussian State Agrarian Technical University, BY-220023 Minsk, Belarus
[5] Institute of Physics, Polish Academy of Sciences, PL-02-668 Warsaw, Poland

E-mail: sazonov@ifttp.bas-net.by

Received 16 February 2005, in final form 20 May 2005
Published 17 June 2005
Online at stacks.iop.org/JPhysCM/17/4181

Abstract

The properties of $Nd_{1-x}Ba_xCoO_3$ ($0 \leqslant x \leqslant 0.24$) solid solutions were studied at non-ambient temperatures by x-ray and neutron powder diffraction methods as well as magnetization and resistivity measurements. All the samples have an orthorhombically distorted perovskite structure (*Pbnm* space group). It was found that compositions with $x \leqslant 0.06$ exhibit paramagnetic behaviour down to liquid helium temperature, and those with $0.08 \leqslant x \leqslant 0.16$ are spin glasses, whereas both long-range ferromagnetic order ($T_C \sim 130$ K) and metallicity above T_C seem to occur simultaneously at $x \geqslant 0.18$. According to neutron diffraction data at different temperatures ($T = 3$–540 K), there are no crystal structure anomalies associated with orbital ordering of the Co^{3+} ions in the intermediate-spin state for $NdCoO_3$. This is in agreement with gradual thermal excitation of the Co^{3+} ions from low- to intermediate- or high-spin state in a wide temperature range up to a metal–insulator transition (~600 K). The possible mechanisms of magnetic interactions are discussed.

1. Introduction

$La_{1-x}M_xCoO_3$ (M—alkaline-earth metal) solid solutions attract much attention of researchers due to the possibility of application as magnetic media, cathode materials, catalysts, etc. Moreover, these systems are interesting because of their unusual properties, such as the appearance of both ferromagnetism and metallicity by doping or increasing temperature, and spin state transitions of the Co ions. It is worth noting that Co ions can be in low-spin (LS;

[6] Author to whom any correspondence should be addressed.

0953-8984/05/264181+15$30.00

t_{2g}^6, $S = 0$), intermediate-spin (IS; $t_{2g}^5 e_g^1$, $S = 1$) and high-spin (HS; $t_{2g}^4 e_g^2$, $S = 2$) electronic configurations due to a competition between crystal-field energy and Hund (intra-atomic) exchange energy. For instance, in $LaCoO_3$, substitution of La^{3+} for Sr^{2+} leads to the formation of the tetravalent Co^{4+} ions as well as stabilization of the Co^{3+} ions in the IS state [1]. These effects modify both the crystal and magnetic structures of the parent compound, and positive exchange interactions Co^{3+}–O–Co^{4+} establish long-range ferromagnetic order at $x \approx 0.18$ [2].

It was originally supposed that the mechanism of exchange interactions in the cobaltites is the same as for the manganites [3]. Therefore, the magnetic properties of the $La_{1-x}Sr_xCoO_3$ system were interpreted by the mechanism of double exchange interactions between Co^{3+} and Co^{4+} ions [3] by analogy to the more investigated manganites. However, Goodenough has suggested [4] that the magnetic properties of the cobaltites can be explained by superexchange interaction through the anions without the double exchange. Subsequently, the ferromagnetic properties of the $La_{1-x}Sr_xCoO_3$ system were explained by Goodenough in a model of itinerant-electron ferromagnetism [5]. Nevertheless, the origin of the exchange interactions both in the cobaltites and manganites is still a subject of discussion. At present, the majority of researchers assume that the double exchange is responsible for ferromagnetic properties of the manganites. Moreover, there is evidence to suggest that the origin of exchange interactions in the cobaltites differs from that in the manganites. Thus, the metal–insulator (MI) transition and the appearance of long-range ferromagnetic order are separated from each other in the manganites. For instance, in the $La_{1-x}Ca_xMnO_3$ system, the transition into the ferromagnetic state occurs at $x \approx 0.1$, whereas the metallic behaviour appears only for $x \gtrsim 0.22$ [6]. On the other hand, it is impossible to separate the transitions to ferromagnetic and metallic states in the $La_{1-x}Sr_xCoO_3$ system and these transitions coincide in the temperature–composition phase diagram [7]. It is also worth noting that a metal–insulator transition in the manganites was observed at about the temperature of ferromagnetic ordering (T_C) [8, 9], in contrast with the cobaltites. For instance, the character of conductivity does not change at T_C for the metallic $La_{1-x}Sr_xCoO_3$ [2, 7] and $La_{1-x}Ca_xCoO_3$ [10] systems, and only a break point on the resistivity–T curve is observed. Magnetoresistive properties of the cobaltites and manganites also differ noticeably. In the manganites the highest magnetoresistance (MR) is connected with the MI transition and is observed near the Curie temperature [11, 12]. For instance, the MR of $La_{0.88}MnO_{2.94}$ in 0.9 T near T_C (∼250 K) is about 90% [11]. On the other hand, in the $La_{1-x}Sr_xCoO_3$ system [13] such an MR peak is very small ($x = 0.18$, $H = 7$ T, MR $\approx$ 10%). Moreover, in the spin glass state ($x < 0.18$) an increase of MR is observed with decreasing temperature and the maximum at liquid helium temperature is five times larger ($x = 0.15$, $H = 7$ T, MR $\approx$ 50%) than that observed near the ferromagnetic transition. Finally, the intergranular MR at small magnetic field (∼5 kOe) is found only in the polycrystalline manganites.

In addition, there is no clarity on the spin state of the Co ions in the cobaltites at different temperatures. It was primarily assumed that the spin state transition of the Co^{3+} ions from the LS to the HS state occurs near 100 K [4, 14–16]. However, using the LDA + U (local density approximation plus Hubbard model approach) method, Korotin *et al* [17] proposed that the energy of the IS state is a little higher than that of the LS state and much lower than the energy of the HS state. They concluded that the orbital ordering of the Co^{3+} ions could be due to the Jahn–Teller (JT) nature of the cobalt ions in the IS state. A cooperative JT distortion has been also suggested by significant changing of Co–O distances evidenced with x-ray diffraction measurements [18]. According to recent spectroscopy studies [19–21], a gradual changing of Co spin state with increasing temperature starts at about 50–120 K.

It is known that the properties of compounds with the perovskite structure change noticeably with replacement of the La ion by another rare-earth (RE) element with smaller

ionic radius. For the $RECoO_3$ (RE—Pr, Nd and Eu) compounds the temperatures of the spin state transition were supposed to be below room temperature [22, 23]. However, both nuclear magnetic resonance (NMR) and magnetic studies [24, 25] of $RECoO_3$ (RE—Pr, Nd, Sm and Eu) indicate that the Co ions remain in the LS state up to the temperature of the metal–insulator transition (∼600 K). Thus, theoretical [26] and experimental [24, 25, 27, 28] data show the LS state of the Co ions to be more stable in such compounds as compared with the lanthanum cobaltites. Moreover, there are few experimental data for such systems doped by Ba ions [29–32], especially with RE = Nd [31, 32].

In the present paper we report the results of a study of the $Nd_{1-x}Ba_xCoO_3$ ($0 \leqslant x \leqslant 0.24$) system by x-ray and neutron powder diffraction methods as well as magnetization and resistivity measurements. According to our previous studies [31, 32], orthorhombically (*Pbnm* space group [33]) distorted $Nd_{1-x}Ba_xCoO_3$ solid solutions exist up to $x = 0.3$. With more Ba ($x \geqslant 0.46$), the solids suffer tetragonal distortion ($P4/mmm$ space group [33]) which are caused by spatial ordering of Nd^{3+} and Ba^{2+} ions, whereas this system exists in the two-phase state in the composition range $0.3 < x < 0.46$. In the present work, we therefore investigated the structural, magnetic, electrical properties of solids with low Ba concentrations. Our aims were: (1) to determine the concentration at which the long-range ferromagnetic order occurs in the $Nd_{1-x}Ba_xCoO_3$ system; (2) to elucidate whether the transition to the ferromagnetic state coincides with the metal–insulator one in this system; (3) to establish the crystal structure peculiarities (if any) associated with change of the Co^{3+} ions' spin state from LS to IS in this system.

2. Experiment

$Nd_{1-x}Ba_xCoO_3$ ($0 \leqslant x \leqslant 0.24$; $\Delta x = 0.02$) solid solutions were synthesized by the conventional ceramic method. Starting powders of Nd_2O_3, Co_3O_4 and $BaCO_3$ were mixed in stoichiometric proportions, pressed into pellets and heated at 1000 °C for 12 h in air. The pellets were then ground, re-pressed and sintered at 1200 °C for 24 h in air. After synthesis the samples were slowly cooled to room temperature at a rate of 50 °C h^{-1} to ensure more complete absorption of oxygen by the lattice. To remove internal residual stresses the samples to be investigated were then annealed at 1000 °C in air. The oxygen content in the samples was determined using thermogravimetric analysis (TGA). A number of samples were annealed in evacuated silica tubes at 800 °C for a long time. Metallic tantalum was used as a reducing agent. As a result of such a procedure all the samples were completely reduced to a mixture of Nd_2O_3, BaO and Co metal.

Electrical conductivity was measured in the temperature range from 80 to 300 K by a standard four-probe method, with indium contacts formed by ultrasonic soldering. Magnetization measurements were performed using a commercial vibrating sample magnetometer OI-3001. The temperature dependences of the magnetization $M(T)$ were measured on warming from 4 to 250 K in a field of 100 Oe after a field cooling (FC) or zero field cooling (ZFC) procedure. The field dependence of magnetization $M(H)$ was measured at 4.2 K after a field cooling procedure. The identification of all the phases at room temperature was performed using a DRON-3M powder x-ray diffractometer with Cu Kα radiation. The neutron powder-diffraction experiments for the $NdCoO_3$ and $Nd_{0.78}Ba_{0.22}CoO_3$ samples were carried out on the fine resolution powder diffractometer (FIREPOD) of the Berlin Neutron Scattering Center (BENSC) with incident neutrons of wavelength $\lambda = 1.7973(1)$ Å. Data were collected on warming from 3 to 540 K in the angular range of $10° < 2\Theta < 150°$. The neutron and x-ray powder diffraction data of all the samples at different temperatures have been analysed with the Rietveld method [34] using the FullProf program [35].

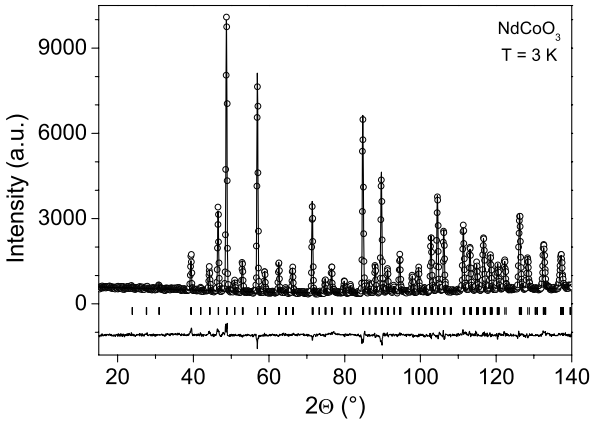

Figure 1. Results of the Rietveld refinement of the neutron powder diffraction pattern of $NdCoO_3$ measured at 3 K. The measured data (open circles) are shown together with the resulting fit (continuous line) and their difference plot (continuous line below). The ticks show the 2Θ positions for the Bragg peaks of the orthorhombic (*Pbnm* space group) crystal phase.

Table 1. The unit cell parameters and volume of the $Nd_{1-x}Ba_xCoO_3$ system in the orthorhombic *Pbnm* space group for different values of x.

x	a (Å)	b (Å)	c (Å)	V (Å^3)
0	5.3460(7)	5.3363(7)	7.5455(5)	215.26(4)
0.04	5.3694(2)	5.3501(4)	7.5691(7)	217.44(9)
0.06	5.3742(9)	5.3549(3)	7.5767(5)	218.04(4)
0.08	5.3813(7)	5.3581(7)	7.5894(4)	218.83(4)
0.10	5.3892(7)	5.3632(7)	7.6004(4)	219.68(4)
0.12	5.3938(7)	5.3680(7)	7.6085(5)	220.30(4)
0.14	5.4032(7)	5.3764(5)	7.6130(5)	221.16(4)
0.16	5.4088(7)	5.3794(7)	7.6143(6)	221.55(4)
0.18	5.4169(4)	5.3830(5)	7.6173(5)	222.11(3)
0.20	5.4214(4)	5.3875(5)	7.6207(5)	222.58(3)
0.22	5.4266(7)	5.3921(7)	7.6282(4)	223.21(5)
0.24	5.4333(7)	5.3956(7)	7.6303(8)	223.69(5)

3. Results

3.1. Structural studies

Structural studies of all the samples at room temperature were carried out using x-ray diffraction data, and the crystal structure is confirmed to be orthorhombic (*Pbnm* space group [33]). The unit cell parameters as well as the volume at room temperature were found to gradually increase with Ba content (table 1). We also have obtained neutron diffraction pattern of $NdCoO_3$ and $Nd_{0.78}Ba_{0.22}CoO_3$ at 3, 120, 300, 540 K and 4, 120, 300 K, respectively. The refinement results of the crystal structure at room temperature are in agreement with those obtained from x-ray analysis. Structural parameters, Co–O distances and Co–O–Co angles determined by Rietveld refinement as well as reliability factors (R) for the fitting are reported in tables 2 and 3 for $NdCoO_3$ and $Nd_{0.78}Ba_{0.22}CoO_3$, respectively. It is worth noting that both the unit cell parameters and volume of these samples also increase with temperature (tables 2 and 3). The results of Rietveld refinement of both samples at low temperatures are presented in figures 1 and 2 for $NdCoO_3$ and $Nd_{0.78}Ba_{0.22}CoO_3$, respectively. The temperature dependences

Table 2. Results of Rietveld refinement of neutron diffraction data for $NdCoO_3$ in space group *Pbnm* at different temperatures. Atomic positions: Nd—4c(x, y, $\frac{1}{4}$); Co—4b($\frac{1}{2}$, 0, 0); O(1)—4c(x, y, $\frac{1}{4}$); O(2)—8d(x, y, z).

		T (K)			
		3	120	300	540
a (Å)		5.3331(1)	5.3343(1)	5.3429(1)	5.3721(2)
b (Å)		5.3292(1)	5.3302(1)	5.3367(1)	5.3717(2)
c (Å)		7.5364(2)	7.5375(1)	7.5486(2)	7.5942(3)
V (Å^3)		214.19(1)	214.31(1)	215.24(1)	219.15(1)
Nd:	x	0.9912(7)	0.9911(6)	0.9909(5)	0.9914(11)
	y	0.0367(4)	0.0376(4)	0.0340(4)	0.0335(7)
	z	1/4	1/4	1/4	1/4
Co:	x	1/2	1/2	1/2	1/2
	y	0	0	0	0
	z	0	0	0	0
O(1):	x	0.0717(10)	0.0731(9)	0.0711(9)	0.0747(17)
	y	0.4914(6)	0.4915(5)	0.4923(6)	0.4911(11)
	z	1/4	1/4	1/4	1/4
O(2):	x	0.7130(6)	0.7134(5)	0.7140(5)	0.7136(9)
	y	0.2874(5)	0.2866(6)	0.2860(5)	0.2850(11)
	z	0.0377(4)	0.0369(4)	0.0370(4)	0.0356(7)
R_p (%)		4.60	4.62	4.26	5.21
R_{wp} (%)		5.83	5.83	5.39	6.68
R_{exp} (%)		3.74	3.74	3.72	3.73
R_B (%)		6.76	6.77	6.74	7.60
χ^2 (%)		2.44	2.42	2.10	3.40
Co–O(1) (Å) × 2		1.924(4)	1.926(3)	1.928(3)	1.932(5)
Co–O(2) (Å) × 2		1.927(3)	1.926(4)	1.925(4)	1.925(4)
Co–O(2) (Å) × 2		1.928(3)	1.927(3)	1.929(4)	1.958(5)
⟨Co–O⟩ (Å)		1.9263	1.9263	1.9273	1.9383
Co–O(1)–Co (deg)		155.86(5)	155.96(5)	156.43(5)	156.08(8)
Co–O(2)–Co (deg)		156.54(2)	156.45(2)	157.33(1)	158.38(3)

of the Co–O lengths and Co–O–Co angles of $RE_{1-x}M_xCoO_3$ are shown in figures 3 and 4, respectively. The literature values [1, 18, 36, 37] are shown together with the present data.

The results indicate that the general trend of the thermal expansion appears to be normal; the cell parameters and cell volume increase with temperature for both $NdCoO_3$ and $Nd_{0.78}Ba_{0.22}CoO_3$ samples. Moreover, there are no significant anomalies in the Co–O bond lengths at measured temperatures up to 300 K for both samples. In this temperature range the bond lengths are close to each other for $NdCoO_3$, and rather appreciable distortions of oxygen octahedrons were observed only at high temperature ($T = 540$ K). On the other hand, for the $Nd_{0.78}Ba_{0.22}CoO_3$ sample the CoO_6 octahedrons are rather distorted even at 4 K, and the average ⟨Co–O⟩ bond length gradually increases with temperature (table 3). One of the Co–O bond lengths and one of the Co–O–Co bond angles contract with increasing temperature. This is probably due to an increase of distortion of oxygen octahedrons associated with stabilization of the Co^{3+} ions in the intermediate-spin state. The investigation of any subtle changes should be performed with smaller temperature steps, but this is outside the scope of the present work.

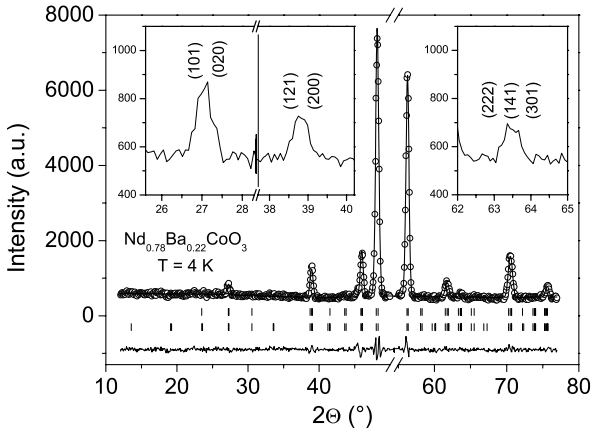

Figure 2. Results of the Rietveld refinement of the neutron powder diffraction pattern of $Nd_{0.78}Ba_{0.22}CoO_3$ measured at 4 K. The measured data (open circles) are shown together with the resulting fit (continuous line) and their difference plot (continuous line below). The ticks show the 2Θ positions for the Bragg peaks of the orthorhombic (*Pbnm* space group) crystal phase (upper row) and the magnetic phase (lower row). The plots in the insets show some magnetic contributions into peaks revealed by subtracting the pattern measured at 4 K from that at 300 K.

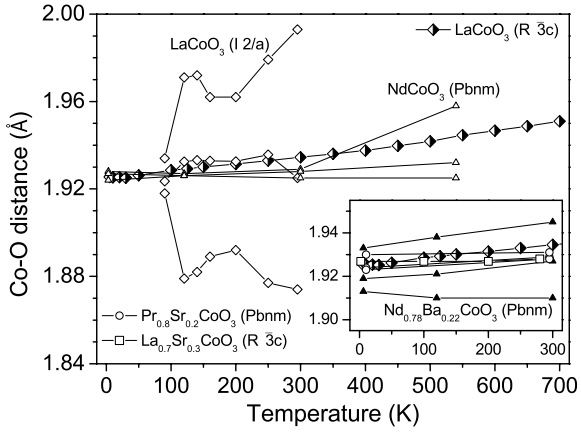

Figure 3. The temperature dependences of the Co–O bond lengths of $LaCoO_3$ ($I2/a$ [18] and $R\bar{3}c$ [37] space groups) and $NdCoO_3$ ($Pbnm$). The plot in the inset shows the temperature dependences of the Co–O bond lengths of $Nd_{0.78}Ba_{0.22}CoO_3$ ($Pbnm$), $Pr_{0.8}Sr_{0.2}CoO_3$ ($Pbnm$) [36] and $La_{0.8}Sr_{0.2}CoO_3$ ($R\bar{3}c$) [1].

3.2. Magnetic properties

According to the magnetization measurements for the $Nd_{1-x}Ba_xCoO_3$ system in $0 \leqslant x \leqslant 0.24$ there are three composition ranges with different magnetic behaviour. Figures 5 and 6 show the temperature dependences of the ZFC ($M_{ZFC}(T)$) and FC ($M_{FC}(T)$) magnetization. The reciprocal magnetization ($1/M$) and field-dependent magnetization ($M(H)$) are presented in figures 8 and 7, respectively.

3.2.1. $0.00 \leqslant x \leqslant 0.06$. As can be seen in figure 5, the $M_{FC}(T)$ and $M_{ZFC}(T)$ curves practically coincide in all the temperature range. All the magnetization curves exhibit a

Table 3. Results of Rietveld refinement of neutron diffraction data for $Nd_{0.78}Ba_{0.22}CoO_3$ in space group *Pbnm* at different temperatures. Atomic positions: Nd/Ba—4c(x, y, $\frac{1}{4}$); Co—4b($\frac{1}{2}$, 0, 0); O(1)—4c(x, y, $\frac{1}{4}$); O(2)—8d(x, y, z).

		T (K)		
		4	120	300
a (Å)		5.4143(2)	5.4164(2)	5.4287(2)
b (Å)		5.3746(2)	5.3774(2)	5.3916(2)
c (Å)		7.6044(2)	7.6072(3)	7.6299(3)
V (Å^3)		221.29(1)	221.57(2)	223.40(2)
Nd/Ba:	x	0.9979(8)	0.9973(9)	0.9999(10)
	y	0.0037(15)	0.0039(17)	0.0024(21)
	z	1/4	1/4	1/4
Co:	x	1/2	1/2	1/2
	y	0	0	0
	z	0	0	0
O(1):	x	0.0474(10)	0.0492(10)	0.0489(13)
	y	0.4895(28)	0.4926(24)	0.5125(36)
	z	1/4	1/4	1/4
O(2):	x	0.7416(22)	0.7420(20)	0.7430(25)
	y	0.2612(20)	0.2624(17)	0.2619(19)
	z	0.0306(5)	0.0302(5)	0.0294(5)
R_p (%)		5.22	5.32	5.26
R_{wp} (%)		6.33	6.41	6.39
R_{exp} (%)		3.69	3.74	3.65
R_B (%)		7.56	7.77	7.62
χ^2 (%)		3.04	3.22	3.19
Co–O(1) (Å) × 2		1.913(2)	1.910(2)	1.910(3)
Co–O(2) (Å) × 2		1.919(5)	1.921(5)	1.927(5)
Co–O(2) (Å) × 2		1.933(4)	1.938(5)	1.945(5)
⟨Co–O⟩ (Å)		1.921	1.923	1.927
Co–O(1)–Co (deg)		164.26(5)	163.87(6)	163.66(7)
Co–O(2)–Co (deg)		165.39(3)	165.51(3)	165.95(3)

typically paramagnetic behaviour. We think that the increase of magnetization with decreasing temperature is mainly due to the paramagnetic Nd^{3+} ions. This is probably because of rather weak magnetic interactions between Co ions which are masked by the Nd magnetic moments contribution.

3.2.2. $0.08 \leqslant x \leqslant 0.16$. A doping of Ba above $x \sim 0.07$ leads to several changes in magnetic properties as mentioned below. The magnetization versus temperature curves can be interpreted in terms of a spin glass (SG). In the $M_{ZFC}(T)$ curves a plateau appears at ∼12 K ($x = 0.08$), and a cusp is seen for $x > 0.08$. This cusp probably marks the freezing temperature T_f of magnetic moments of the Co ions (figure 5) that are associated with the transition in the SG state. The plateau for $x = 0.08$ results from competition between neodymium and cobalt contributions. T_f gradually increases with increasing Ba concentration. The shape of the $1/M$ curves changes for the compounds with $x \geqslant 0.08$ (figure 8). The field dependences of magnetization $M(H)$ for these samples demonstrate that no saturation occurs up to 15 kOe, and indicate a high coercivity H_C up to 11 kOe (figure 7). However, it is worth noting that

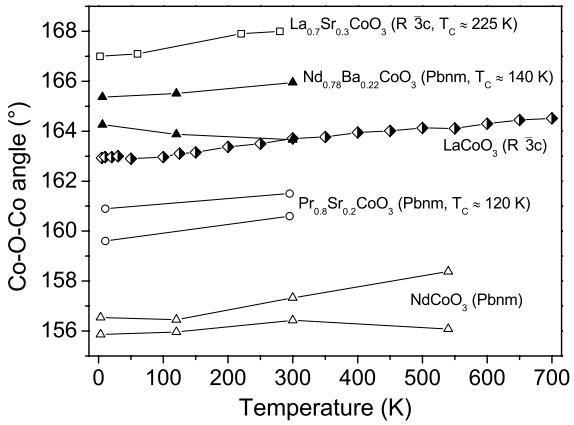

Figure 4. The temperature dependences of the Co–O–O bond angles of $LaCoO_3$ ($R\bar{3}c$ [37] space group), $NdCoO_3$ ($Pbnm$), $Nd_{0.78}Ba_{0.22}CoO_3$ ($Pbnm$), $Pr_{0.8}Sr_{0.2}CoO_3$ ($Pbnm$) [36] and $La_{0.8}Sr_{0.2}CoO_3$ ($R\bar{3}c$) [1].

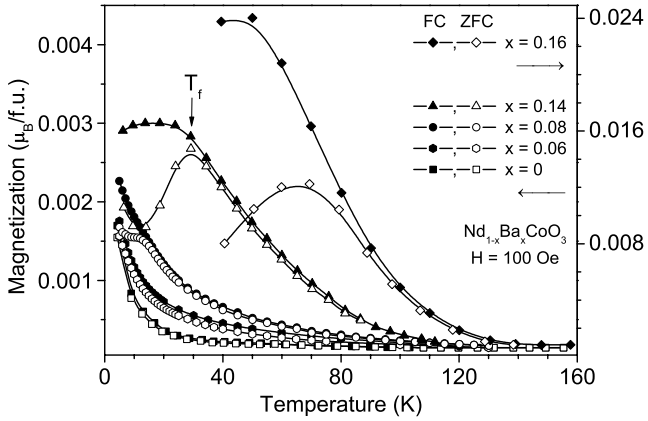

Figure 5. Temperature dependences of the magnetization of the $Nd_{1-x}Ba_xCoO_3$ ($0 \leqslant x \leqslant 0.16$) compounds measured in a field of 100 Oe after an FC or ZFC procedure.

the additional investigations, like measurements of the relaxation time of magnetization, is necessary to prove the SG state.

3.2.3. $0.18 \leqslant x \leqslant 0.24$. Further increasing the Ba concentration over $x \sim 0.17$ introduces a magnetic phase different from the spin glass one. The samples with $x > 0.18$ have a rather high spontaneous magnetization (figure 7) and a much sharper transition to a paramagnetic state (figures 6 and 8) compared with samples with lower Ba concentration. The coercivity H_C drops abruptly down to ~6 kOe for the sample with $x = 0.22$. Apparently $x \approx 0.18$ is the magnetic percolation threshold, and for $x \geqslant 0.18$ long-range ferromagnetic order occurs by analogy to the $La_{1-x}Sr_xCoO_3$ system [2]. The Curie point weakly depends on the Ba concentration, as can be seen from figure 6.

For these samples the $M_{ZFC}(T)$ curve deviates from $M_{FC}(T)$ slightly below T_C, passes through a maximum and then exhibits a gradual reduction with decreasing temperature. Such a behaviour of $M_{ZFC}(T)$ is characteristic of the cobaltites and lightly doped manganites and is

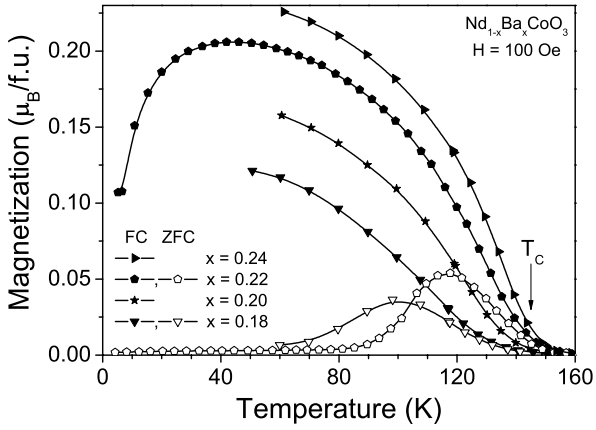

Figure 6. Temperature dependences of the magnetization of the $Nd_{1-x}Ba_xCoO_3$ ($0.18 \leqslant x \leqslant 0.24$) compounds measured in a field of 100 Oe after an FC or ZFC procedure. The plot in the inset shows the changing of the form of $M(T)$ curves for the compounds with $x \geqslant 0.18$.

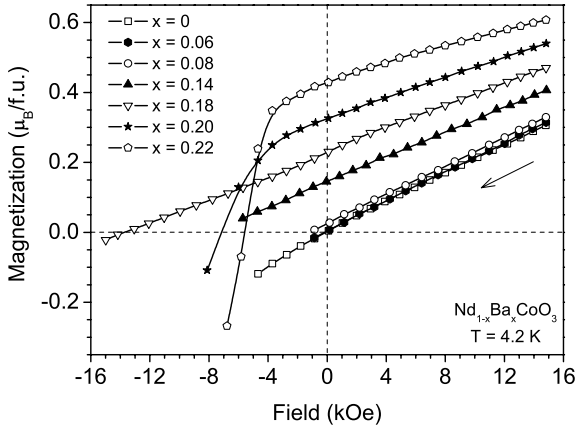

Figure 7. The field dependences of magnetization of the $Nd_{1-x}Ba_xCoO_3$ ($0 \leqslant x \leqslant 0.22$) compounds measured at temperature of 4.2 K.

attributed to the large magnetic anisotropy of these compounds [38]. The saturation of $M(H)$ is also not achieved up to 15 kOe, where the magnetic moment per formula unit is about 0.6 μ_B for the $Nd_{0.78}Ba_{0.22}CoO_3$ compound (figure 7). The magnetic moment of the Co sublattice (M_{Co}) is difficult to determine because of the negative f–d magnetic interaction orienting the magnetic moment of the Nd sublattice in the opposite direction to that of the Co one. The sharp decrease of $M_{FC}(T)$ below ~40 K for $Nd_{0.78}Ba_{0.22}CoO_3$ (figure 6) probably corresponds to antiparallel ordering of the Nd ions towards Co ones.

From neutron diffraction studies of the $NdCoO_3$ and $Nd_{0.78}Ba_{0.22}CoO_3$ samples, a magnetic contribution to Bragg peaks was found only for the latter, which is in agreement with magnetization measurements. The growth in the intensity of magnetic reflections with temperature for the $Nd_{0.78}Ba_{0.22}CoO_3$ sample is most evident for the peaks shown in the inset of figure 2. No magnetic satellites corresponding to any antiferromagnetic type of order have been detected in both samples at least down to 3 K. To determine the magnetic moment of the Co sublattice from our neutron diffraction measurement we assumed that the Nd sublattice is

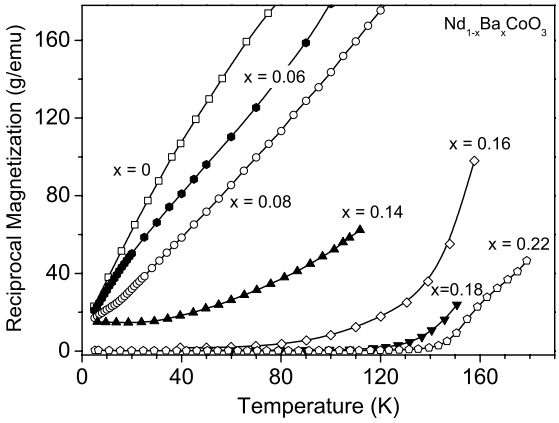

Figure 8. Temperature dependences of the reciprocal magnetization of the $Nd_{1-x}Ba_xCoO_3$ ($0 \leqslant x \leqslant 0.24$) compounds.

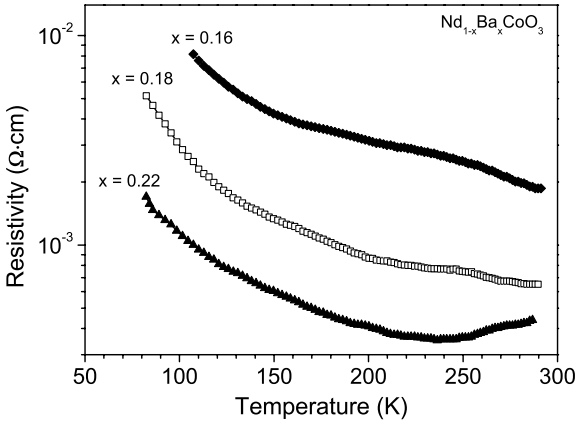

Figure 9. The temperature dependences of the electrical resistivity of $Nd_{1-x}Ba_xCoO_3$ for $x = 0.16$, 0.18 and 0.22.

ordered with magnetic moment $M_{Nd} \approx 0.8\ \mu_B$ at liquid helium temperature. Such a value of M_{Nd} per Nd ion was obtained from the neutron diffraction data for $Nd_{0.67}Sr_{0.33}CoO_3$ [39]. Thus, at fixed $M_{Nd} \approx 0.8\ \mu_B$ we have obtained the value $M_{Co} \approx 1.25\ \mu_B$ from Rietveld refinement of the magnetic contribution for $Nd_{0.78}Ba_{0.22}CoO_3$ at 4 K. The calculated M_{Co} value for the IS Co^{3+} ($t_{2g}^5e_g^1$, $S = 1$) and LS Co^{4+} (t_{2g}^5, $S = 1/2$) is about 1.8 μ_B per Co ion. One can therefore suggest that some part of the trivalent cobalt ions is in the LS state.

3.3. Electrical measurements

Figure 9 shows the temperature dependences of the electrical resistivity of $Nd_{1-x}Ba_xCoO_3$ for $x = 0.16$, 0.18 and 0.22 in the temperature range from 80 to 300 K. In general, the resistivity of the samples decreases as the doping level increases. For $x = 0.16$ and 0.18, the samples show semiconductor behaviour up to room temperature, with ρ values from 10^{-3} to $10^{-2}\ \Omega$ cm, whereas the resistivity of the sample with $x = 0.22$ exhibits rather complex behaviour. It decreases with increasing temperature from 80 K (similar to $x = 0.16$ and 0.18),

passes through a minimum at about 235 K and then increases, which corresponds to metallic behaviour. Thus, substitution of Nd for Ba leads to changing the conductive mechanism above T_C from semiconductor ($x < 0.20$) to metal-like ($x > 0.20$).

4. Discussion

4.1. Spin state of Co ions

As was pointed out in the introduction, the authors of [18] carried out x-ray diffraction measurements of $LaCoO_3$ to detect lattice distortions due to the JT effect. They took into account that the cooperative JT distortion is incompatible with the $R\bar{3}c$ space group (rhombohedral symmetry) which preserves only one oxygen position and Co–O distance. Therefore, they concluded that it is necessary to lower the symmetry to the monoclinic one with the $I2/a$ space group (a subgroup of $R\bar{3}c$) and two non-equivalent O positions. Refinement in the monoclinic space group showed a significant change of Co–O distances near 100 K and it was associated with the cooperative orbital ordering.

However, it is well known that, in the presence of heavy atoms, small displacements of the oxygen positions can be difficult to detect with accuracy by x-ray diffraction. For this type of problem neutron diffraction has an advantage, because neutrons interact directly with atomic nuclei and the neutron scattering length varies non-monotonically and thus light atoms can be localized as easily as heavy ones [40]. Moreover, a number of neutron diffraction data of $LaCoO_3$ [37, 41, 42] were reasonably well refined in the $R\bar{3}c$ space group. Our neutron diffraction data of the $NdCoO_3$ compound were refined in the orthorhombic $Pbnm$ space group with two non-equivalent oxygen positions.

According to our data there are no significant anomalies in the temperature dependences of the Co–O distances up to 540 K (figure 3, table 2). The Co–O bond lengths in $NdCoO_3$ are rather close to each other, which is incompatible with cooperative orbital ordering of the JT Co^{3+} ions in the IS state, and only local JT distortion is possible thereby. Rather appreciable distortions of oxygen octahedrons CoO_6 were observed only near the $T_{MI} \sim 600$ K, which suggests increasing concentration of the Co^{3+} ions in the intermediate-spin state. The average ⟨Co–O⟩ bond length in $NdCoO_3$ is smaller than that in $LaCoO_3$ (figure 3). This fact is in agreement with a greater stability of the LS Co^{3+} ions in $NdCoO_3$ compared with that in $LaCoO_3$, because the ionic radius of Co^{3+} in the LS state is less than that in the IS state [37]. On the other hand, substitution of Nd^{3+} for Ba^{2+} leads to the formation of the tetravalent Co^{4+} ions as well as stabilization of the Co^{3+} ions in the intermediate-spin state [1]; and for the $Nd_{0.78}Ba_{0.22}CoO_3$ sample the CoO_6 octahedrons are distorted even at 4 K (figure 3). However, part of Co^{3+} ions probably exist in the LS state even down to liquid helium temperature, which is in agreement with the small value of the experimental M_{Co} (1.25 μ_B/Co ion) compared to the calculated one (1.8 μ_B/Co ion) for IS Co^{3+} and LS Co^{4+} ions.

It is known that in the cobaltites the crystal-field energy is close to the Hund exchange energy; therefore the spin state transition of Co ions is possible in such materials [43]. The ground state of the cobalt ions can be changed by temperature, doping, external pressure, etc. Factors increasing the Co–O bond lengths lead to the stabilization of IS Co^{3+}, and in contrast factors favouring a decrease of these lengths stabilize Co^{3+} in the LS state. The experimental data indicate that both in $LaCoO_3$ and in $RECoO_3$ (RE—rare-earth element different from La) there is not a phase transition but gradual thermal excitation of Co^{3+} ions from the low-spin state to the intermediate-spin state up to the MI transition temperature. That is, the higher the temperature the more the Co^{3+} ions change their spin state. For instance, according to x-ray emission spectroscopy data for $LaCoO_3$ [19], a change in spin state occurs as the temperature

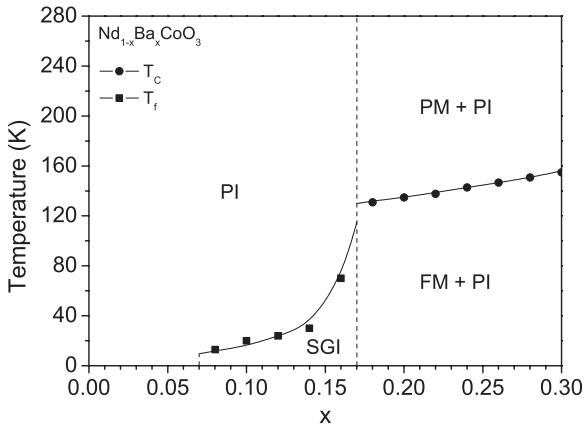

Figure 10. Phase diagram of the $Nd_{1-x}Ba_xCoO_3$ system. SGI—spin glass insulator, FM—ferromagnetic metal, PM—paramagnetic metal, PI—paramagnetic insulator.

is raised from 85 to 300 K. According to the Raman studies of $LaCoO_3$ [20, 21], the presence of the IS Co^{3+} ions above 50–120 K, whose population gradually grows with temperature, was suggested. The closeness and invariability of the Co–O bond lengths in $NdCoO_3$ up to room temperature (figure 3) indicate an appreciable increase of the fraction of Co^{3+} ions in the IS state only above 300 K. This fact is in agreement with the magnetic and NMR measurements [24, 25], according to which weak anomalies were observed on magnetic susceptibility and Knight shift curves only near $T_{MI} \sim 600$ K.

We believe a temperature about 50–120 K to be sufficient for thermal excitation of the Co^{3+} ions in $LaCoO_3$ from the LS to IS/HS state. As for $RECoO_3$ (RE—rare-earth element different from La), such excitation is effective enough only above room temperature; and the ground state of Co^{3+} ions in such systems probably remains LS up to the metal–insulator transition temperature.

4.2. Mechanism of exchange interactions

It was originally supposed that the mechanism of exchange interactions in the cobaltites is the same as for the manganites (see the introduction). However, there are significant differences in properties of the cobaltites and manganites; this is well appreciable with the colossal magnetoresistive effect, for example. Moreover, the MI transition at T_C as well as mismatch of the doping concentrations x at which transition occurs in metallic and ferromagnetic states are observed only in the manganites. On the other hand, in the mixed valence cobaltites ferromagnetism and metallicity are closely connected to each other and established simultaneously in a composition range $x \sim 0.15$–0.20. For instance, it is impossible to separate the transitions to ferromagnetic and metallic states in the $Nd_{1-x}Ba_xCoO_3$ system, and these transitions coincide in the temperature–composition phase diagram (figure 10), similar to other cobaltite systems. This phase diagram has been obtained on the basis of our previous [31, 32] and present studies of the $Nd_{1-x}Ba_xCoO_3$ system.

In figure 11, T_C values versus $\langle r_A \rangle$ (average radius calculated from the radii of A-site ions) in $RE_{0.8}M_{0.2}CoO_3$ are plotted according to our data and literature [44–48]. These results show the important role of cation size for the value of the Curie temperature T_C. As is evident from figure 11, T_C decreases with $\langle r_A \rangle$ value. Decreasing the bond angle Co–O–Co value also leads to decreasing T_C. It is worth noting that in the superexchange model the magnetic interactions

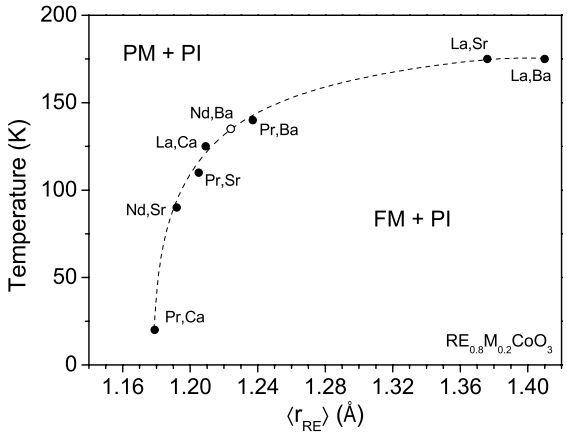

Figure 11. Variation of the Curie temperature T_C with $\langle r_A \rangle$ in $RE_{0.8}M_{0.2}CoO_3$. The data were taken from the literature [1, 18, 36, 37] (closed circles) and from present study (open circle). FM—ferromagnetic metal, PM—paramagnetic metal, PI—paramagnetic insulator. RE and M indicated in the figure. The broken curve is drawn as a guide to the eye.

between Co^{3+} and Co^{4+} ions are changed with replacement of RE element since the bond angle depends on the ionic radius of the RE element. The Goodenough–Kanamori rule predicts the superexchange interaction between IS Co^{3+} and LS Co^{4+} to be positive for 180° and negative for 90° [49].

In contrast to the manganites, none of the considered cobaltites (figure 11) demonstrate a change in character of conductivity near the temperature of ferromagnetic ordering. Only a break point on the resistivity curve is observed for instance for the metallic $La_{1-x}Ca_xCoO_3$ [10] and $La_{1-x}Sr_xCoO_3$ [2] cobaltites, and there are no anomalies in $\rho(T)$ near T_C for $Nd_{1-x}Ba_xCoO_3$ (figure 9). Earlier, we have noted that the magnetoresistance in the cobaltites is much less than that in the manganites (see the introduction).

All the above-mentioned distinctions in properties of the cobaltites and manganites are in agreement with the assumption that the origin of exchange interactions in both families of compounds differs. Therefore, Goodenough has interpreted the magnetic properties of the $La_{1-x}Sr_xCoO_3$ system using a superexchange model [4] in the assumption of the localized 3d electrons. Afterwards, he explained the properties of $La_{1-x}Sr_xCoO_3$ in a model of itinerant-electron ferromagnetism [5], due to the large effect of covalence in perovskite-type oxides [50].

We believe that the classical double exchange model is not applicable for the mixed valence cobaltites and itinerant electrons appropriate for the ferromagnetism in these systems, in which there is a competition between crystal-field energy and Hund exchange energy. On the other hand, the double exchange model is more appropriate for the manganites, for which the Hund exchange interaction is too large compared with the band width and ferromagnetism is observed even in the insulator state.

5. Conclusion

The crystal, magnetic and electrical properties of the $Nd_{1-x}Ba_xCoO_3$ ($0 \leqslant x \leqslant 0.24$) system were determined by x-ray and neutron powder diffraction methods as well as magnetization and resistivity measurements.

The results of crystallographic studies indicate that all the samples have an orthorhombically distorted perovskite structure ($Pbnm$ space group). The unit cell parameters

and volume at room temperature were found to gradually increase with Ba content. The gradual increase is also observed with increasing temperature from 3 to 540 K and from 4 to 300 K for $NdCoO_3$ and $Nd_{0.78}Ba_{0.22}CoO_3$, respectively.

It was found that compounds with $x \leqslant 0.06$ exhibit paramagnetic behaviour down to liquid helium temperature. Compounds with $0.08 \leqslant x \leqslant 0.16$ are spin glasses. The substitution of Nd by about 18–20% Ba ions leads to appearance of long-range ferromagnetic order below T_C ($\sim$130 K). The doping of Ba about $x \approx 0.20$ also leads to changing the conductive mechanism above T_C from a semiconductor to a metal-like one. This is in agreement with the data for other mixed valence cobaltites where ferromagnetism and metallicity are closely connected to each other and established simultaneously in a composition range $x \sim 0.15$–0.20.

It was shown that there is no cooperative orbital ordering of the JT Co^{3+} ions in the IS state, and only local JT distortion is possible thereby. The experimental data are in agreement with the fact that in $NdCoO_3$ there is not a phase transition but a gradual thermal excitation of the Co^{3+} ions from a low-spin state to an intermediate-spin state up to the MI transition temperature. Moreover, experimental data are in agreement with the assumption that the origin of exchange interactions in the cobaltites and manganites differs. We believe that itinerant electrons are necessary for the ferromagnetism in the mixed valence cobaltites, in contrast with the manganites, for which ferromagnetism is observed even in the insulator state.

Acknowledgments

The work was supported by the Fund for Fundamental Research of Belarus (project no. F04MS-004) and Polish Committee for Scientific Research (grant 1 P03B 038 27).

References

[1] Caciuffo R, Rinaldi D, Barucca G, Mira J, Rivas J, Señarís-Rodríguez M A, Radaelli P G, Fiorani D and Goodenough J B 1999 *Phys. Rev.* B **59** 1068
[2] Señarís-Rodríguez M A and Goodenough J B 1995 *J. Solid State Chem.* **118** 323
[3] Jonker G H and Van Santen J H 1953 *Physica* **19** 120
[4] Goodenough J B 1958 *J. Phys. Chem. Solids* **6** 287
[5] Raccah P M and Goodenough J B 1968 *J. Appl. Phys.* **39** 1209
[6] Van Aken B B, Jurchescu O D, Meetsma A, Tomioka Y, Tokura Y and Palstra T T M 2003 *Phys. Rev. Lett.* **90** 066403
[7] Wu J and Leighton C 2003 *Phys. Rev.* B **67** 174408
[8] Lanzara A, Saini N L, Brunelli M, Natali F, Bianconi A, Radaelli P G and Cheong S-W 1998 *Phys. Rev. Lett.* **81** 878
[9] Alexandrov A S and Bratkovsky A M 1999 *Phys. Rev. Lett.* **82** 141
[10] Taguchi H, Shimada M and Koizumi M 1982 *J. Solid State Chem.* **44** 254
[11] Troyanchuk I O, Khomchenko V A, Tovar M, Szymczak H and Bärner K 2004 *Phys. Rev.* B **69** 054432
[12] Urushibara A, Moritomo Y, Arima T, Asamitsu A, Kido G and Tokura Y 1995 *Phys. Rev.* B **51** 14103
[13] Golovanov V, Mihaly L and Moodenbaugh A R 1996 *Phys. Rev.* B **53** 8207
[14] Raccah P M and Goodenough J B 1967 *Phys. Rev.* **155** 932
[15] Naiman C S, Gilmore R, DiBartolo B, Linz A and Santoro R 1965 *J. Appl. Phys.* **36** 1044
[16] Marx R 1980 *Phys. Status Solidi* b **99** 555
[17] Korotin M A, Ezhov S Y, Solovyev I V and Anisimov V I 1996 *Phys. Rev.* B **54** 5309
[18] Maris G, Ren Y, Volotchaev V, Zobel C, Lorenz T and Palstra T T M 2003 *Phys. Rev.* B **67** 224423
[19] Magnuson M, Butorin S M, Såthe C, Nordgren J and Ravindran P 2004 *Europhys. Lett.* **68** 289
[20] Seikh M M, Sudheendra L, Narayana C and Rao C N R 2004 *J. Mol. Struct.* **706** 121
[21] Ishikawa A, Nohara J and Sugai S 2004 *Phys. Rev. Lett.* **93** 136401
[22] Sudheendra L, Seikh M M, Raju A R and Narayana C 2001 *Chem. Phys. Lett.* **340** 275
[23] Chang J Y, Lin B N, Hsu Y Y and Ku H C 2003 *Physica* B **329–333** 826
[24] Itoh M, Mori M, Yamaguchi S and Tokura Y 1999 *Physica* B **259–261** 902

[25] Itoh M, Hashimoto J, Yamaguchi S and Tokura Y 2000 *Physica* B **281/282** 510
[26] Nekrasov I A, Streltsov S V, Korotin M A and Anisimov V I 2003 *Phys. Rev.* B **68** 235113
[27] Demazeau G, Pouchard M and Hagenmuller P 1974 *J. Solid State Chem.* **9** 202
[28] Im Y S, Ryu K H, Kim K H and Yo C H 1997 *J. Phys. Chem. Solids* **58** 2079
[29] Yoshii K, Tsutsui S and Nakamura A 2001 *J. Magn. Magn. Mater.* **226–230** 829
[30] Masuda H, Fujita T, Miyashita T, Soda M, Yasui Y, Kobayashi Y and Sato M 2003 *J. Phys. Soc. Japan* **72** 873
[31] Khalyavin D D, Troyanchuk I O, Kasper N V and Szymczak H 2001 *JETP* **93** 805
[32] Khalyavin D D, Sazonov A P, Troyanchuk I O, Szymczak H and Szymczak R 2003 *Inorg. Mater.* **39** 1092
[33] Hahn T 1995 *International Tables for Crystallography* (London: Kluwer)
[34] Rietveld H M 1969 *J. Appl. Crystallogr.* **2** 65
[35] Rodríguez-Carvajal J L 1992 *Physica* B **55** 192
[36] Brinks H W, Fjellvåg H, Kjekshus A and Hauback B C 1999 *J. Solid State Chem.* **147** 464
[37] Radaelli P G and Cheong S W 2002 *Phys. Rev.* B **66** 094408
[38] Ganguly R, Maignan A, Martin C, Hervieu M and Raveau B 2002 *J. Phys.: Condens. Matter* **14** 8595
[39] Krimmel A, Reehuis M, Paraskevopoulos M, Hemberger J and Loidl A 2001 *Phys. Rev.* B **64** 224404
[40] Bridges C, Greedan J E and Barbier J 2000 *Acta Crystallogr.* B **56** 183
[41] Thornton G, Tofield B C and Hewat A W 1986 *J. Solid State Chem.* **61** 301
[42] Xu S, Moritomo Y, Mori K, Kamiyama T, Saitoh T and Nakamura A 2001 *J. Phys. Soc. Japan* **70** 3296
[43] Stølen S, Grønvold F, Brinks H, Atake T and Mori H 1997 *Phys. Rev.* B **55** 14103
[44] Kriener M, Zobel C, Reichl A, Baier J, Cwik M, Berggold K, Kierspel H, Zabara O, Freimuth A and Lorenz T 2004 *Phys. Rev.* B **69** 094417
[45] Burley J C, Mitchell J F and Short S 2004 *Phys. Rev.* B **69** 054401
[46] Yoshii K and Nakamura A 2000 *Physica* B **281/282** 514
[47] Tsubouchi S, Kyômen T, Itoh M and Oguni M 2004 *Phys. Rev.* B **69** 144406
[48] Stauffer D D and Leighton C 2004 *Phys. Rev.* B **70** 214414
[49] Kanamori J 1959 *J. Phys. Chem. Solids* **10** 87
[50] Goodenough J B 1955 *Phys. Rev.* **100** 564